

The Thermodynamic Properties of Polarized Metallic Nanowire in the Presence of Magnetic Field

G.H. Bordbar, L. Shahsavari and M. Sadeghipour

Physics Department, Shiraz University, Shiraz 71454, Iran

(Received 23 September 2012, Accepted 7 January 2013)

In this article, the second quantization method has been used to investigate some thermodynamic properties of spin-polarized metallic nanowire with radius 5 and 10 nm and infinite length, in the presence of magnetic field at zero temperature. The spin-polarization parameter corresponding to the equilibrium state of the system has been plotted as a function of density for different values of the magnetic field. We have concluded that for the magnetic fields less than 100 T at high densities, the system nearly becomes unpolarized. However, for higher magnetic fields, the system has a substantial spin-polarization, even at high densities. Finally, we have calculated the pressure and incompressibility vs. the density for different values of the magnetic field.

Keywords: Metallic nanowire, Second quantization, Electron gas, Spin-polarization

INTRODUCTION

In recent years, nanostructured magnetic materials, due to their interesting physical properties, are of special interests in nanophysics [1,2]. One of the low-dimensional systems is 1D structures. Their magnetic properties are studied since they are the simplest systems in structural view point [3,4]. Physically, stable magnetic metallic nanowires are of the most important nanostructures, and various techniques have been used to prepare and study them [5,6]. They have potential applications in electronics, optoelectronics and memory devices [7-10]. Magnetic nanowires have several applications in magnetic and electric nanodevices [11-14]. Therefore, they are important materials for data storage and information processing [15,16]. Jin *et al.* [17] showed that the magnetic coercivity for the applied field parallel to the nanowires is larger than that for the applied field perpendicular to the nanowires. Zhang *et al.* [10] investigated the magnetic properties of β -FeOOH nanowire arrays using a SQUID magnetometry. Also, they investigated the size-dependent magnetic properties. Xue *et al.* [18] studied the magnetic properties of nanowire arrays at room temperature using the vibrating sample magnetometer and Mossbauer spectrometer. Tung *et al.* [19] calculated the magnetic and electronic properties of both linear and zigzag

atomic chains of all 3D transition metals using the density functional theory with the generalized gradient approximation. Arantes *et al.* [20] investigated the electronic, structural and magnetic properties of Manganese doped Germanium nanowires using *ab initio* total energy density functional theory calculations.

In our previous papers, we have computed some thermodynamic properties of metallic nanowire in the absence of magnetic field [21]. In present work, we calculate the thermodynamic properties of a metallic nanowire using the degenerate electron gas model with the second quantization method in the presence of magnetic field.

SECOND QUANTIZATION METHOD

We consider a pure homogeneous spin-polarized metallic nanowire composed of spin-up (+) and spin-down (-) electrons in a positive background. We denote the number densities of spin-up and spin-down electrons by $\rho^{(+)}$ and $\rho^{(-)}$, respectively. We introduce the spin-polarization parameter (ξ) as follows,

$$\xi = \frac{\rho^{(+)} - \rho^{(-)}}{\rho} \quad (1)$$

where $-1 \leq \xi \leq 1$, and $\rho = \rho^{(+)} + \rho^{(-)}$ is the total density of system.

*Corresponding author. E-mail: bordbar@susc.ac.ir

Second quantization method is used to calculate the energy of the system [21-24].

In this method, we write the one-body (\hat{O}_1) and two-body (\hat{O}_2) operators in terms of the creation (a^+) and annihilation (a) operators, and then we determine the expectation value of these operators for a many-body system,

$$\hat{O}_1 = \sum_{i=1}^N \hat{O}_1(x_i) = \sum_{k_1 k_2 \lambda_1 \lambda_2} a_{k_1 \lambda_1}^+ \langle k_1 \lambda_1 | \hat{O}_1 | k_2 \lambda_2 \rangle a_{k_2 \lambda_2} \quad (2)$$

$$\begin{aligned} \hat{O}_2 &= \frac{1}{2} \sum_{i,j} \hat{O}_2(x_i, x_j) \\ &= \frac{1}{2} \sum_{k_1 k_2 k_3 k_4 \lambda_1 \lambda_2 \lambda_3 \lambda_4} a_{k_1 \lambda_1}^+ a_{k_2 \lambda_2}^+ \langle k_1 \lambda_1 k_2 \lambda_2 | \hat{O}_2 | k_3 \lambda_3 k_4 \lambda_4 \rangle a_{k_3 \lambda_3} a_{k_4 \lambda_4} \end{aligned} \quad (3)$$

In the absence of magnetic field, the Hamiltonian of the system has the following form [21],

$$\hat{H} = \sum_{i=1}^N T(x_i) + \frac{1}{2} \sum_{i \neq j=1}^N V(x_i, x_j) \quad (4)$$

where T is the kinetic energy and V is the inter-particle interaction potential.

For a nanowire (in the cylindrical coordinates), the single-particle wavefunction is as follows [22],

$$\psi_{lmn}(r, \varphi, z) = \frac{1}{\sqrt{\pi R^2 L J_{m+1}(\gamma_{ml} R)}} J_m(\gamma_{ml} r) e^{im\varphi} e^{ilz} \eta_n \quad (5)$$

where R is the radius, L is the length of nanowire, η_n is the spin wave function, and $J_m(\gamma_{ml} r)$ is the Bessel function of order m . $\kappa_{mn} = \gamma_{ml} R$ determined by boundary condition $J_m(\kappa_{mn} \frac{r}{R}) = 0$. The single-particle states are specified by the quantum numbers m , n and l , where l is the wave number of the free motion of electrons along the axis of the nanowire.

On the other hand, the energy levels are as follows,

$$E_{lmn} = \frac{\hbar^2}{2m_e} (\gamma_{ml}^2 + l^2) \quad (6)$$

For the electron gas model of nanowire, H is written by the following formula,

$$H = \sum_{i=1}^N \frac{p_i^2}{2m} + \frac{1}{2} e^2 \sum_{i \neq j=1}^N \frac{e^{-\mu|\vec{r}_i - \vec{r}_j|}}{|\vec{r}_i - \vec{r}_j|} + H_b + H_{el-b} \quad (7)$$

In above equation, μ is convergence coefficient, where $\mu \rightarrow 0$ in the thermodynamic limit ($L \rightarrow \infty, N \rightarrow \infty$). In Eq. (7), H_b is the background Hamiltonian, and H_{el-b} is the potential corresponding the interaction of electrons with background,

$$H_b = \frac{1}{2} e^2 \iint d\vec{x} d\vec{x}' \rho(\vec{x}) \rho(\vec{x}') \frac{e^{-\mu|\vec{x} - \vec{x}'|}}{|\vec{x} - \vec{x}'|} \quad (8)$$

$$H_{el-b} = -e^2 \sum_{i=1}^N \int d\vec{x} \rho(\vec{x}) \frac{e^{-\mu|\vec{x} - \vec{r}_i|}}{|\vec{x} - \vec{r}_i|} \quad (9)$$

In the thermodynamic limit, H_b and H_{el-b} vanish.

Now, we rewrite the Hamiltonian in terms of a^+ and a as follows,

$$\hat{H} = \hat{H}_0 + \hat{H}_1 \quad (10)$$

Where

$$\begin{aligned} \hat{H}_0 &= \sum_{k_1 k_2 \lambda_1 \lambda_2} a_{k_1 \lambda_1}^+ \langle k_1 \lambda_1 | \frac{p^2}{2m_e} | k_2 \lambda_2 \rangle a_{k_2 \lambda_2} \\ &= \sum_{l, m, n, \lambda_1} \frac{\hbar^2}{2m_e} (\gamma_{ml}^2 + l^2) a_{lmn, \lambda_1}^+ a_{lmn, \lambda_1} \end{aligned} \quad (11)$$

$$\hat{H}_1 = \frac{1}{2} \sum_{k_1 k_2 k_3 k_4 \lambda_1 \lambda_2 \lambda_3 \lambda_4} a_{k_1 \lambda_1}^+ a_{k_2 \lambda_2}^+ \langle k_1 \lambda_1 k_2 \lambda_2 | V | k_3 \lambda_3 k_4 \lambda_4 \rangle a_{k_3 \lambda_3} a_{k_4 \lambda_4} \quad (12)$$

In above equation

$$V = \frac{e^2}{(4\pi\epsilon_0)} \times \frac{e^{-\mu\sqrt{(r_1 - r_2)^2 + (z_1 - z_2)^2}}}{\sqrt{(r_1 - r_2)^2 + (z_1 - z_2)^2}} \quad (13)$$

Each k_i denotes to m_i, n_i, l_i . \hat{H}_0 is the unperturbed Hamiltonian that representative of a non-interacting Fermi system, and \hat{H}_1 is considered as the perturbation term.

Now, we calculate the matrix elements in Eq. (11) as follows,

$$\begin{aligned}
 PE &= \langle k_1 \lambda_1 k_2 \lambda_2 | V | k_3 \lambda_3 k_4 \lambda_4 \rangle \\
 &= \frac{e^2}{(4\pi\epsilon_0)\pi^2 R^4 L^2} \times \frac{1}{J_{m_1+1}(\gamma_{m_1 n_1} R) J_{m_2+1}(\gamma_{m_2 n_2} R) J_{m_3+1}(\gamma_{m_3 n_3} R) J_{m_4+1}(\gamma_{m_4 n_4} R)} \\
 &\times \delta_{\lambda_1 \lambda_3} \delta_{\lambda_2 \lambda_4} \times (2\pi)^2 \delta_{m_1 m_3} \delta_{m_2 m_4} \\
 &\times \int_0^R J_{m_1}(\gamma_{m_1 n_1} r_1) J_{m_3}(\gamma_{m_3 n_3} r_1) dr_1 \\
 &\times \int_0^{2R} (r_1 - r) J_{m_2}(\gamma_{m_2 n_2} (r_1 - r)) J_{m_4}(\gamma_{m_4 n_4} (r_1 - r)) \left[L \delta_{l_1+l_2, l_3+l_4} 2K_0 \left(r \sqrt{\mu^2 + (l_2 - l_4)^2} \right) \right] dr
 \end{aligned} \tag{14}$$

where $r = r_1 - r_2$, and $K_0(x)$ is the modified Bessel function of second kind.

We can solve above integrals numerically by Simpson method in Maple software. Finally, we consider the system in the thermodynamic limit ($\mu \rightarrow 0$) [21].

Now we consider the case in which the spin-polarized metallic nanowire is under the influence of a strong magnetic field. Taking the uniform magnetic field along the z direction, $\vec{B} = B\hat{k}$, the spin-up and spin-down particles correspond to parallel and antiparallel spins with respect to the magnetic field. Therefore, the contribution of the magnetic energy of the metallic nanowire is

$$E_M = -M_z B \tag{15}$$

where M_z is the magnetization of metallic nanowire, which is given by

$$M_z = N\mu_e \xi \tag{16}$$

In the preceding equation, $\mu_e = 928.476377 \times 10^{-26} \frac{J}{T}$ is the electron magnetic moment. Using the perturbation theory for the ground state energy (E), we have

$$E = E^{(0)} + E^{(1)} + E_M \tag{17}$$

Where

$$E^{(0)} = \langle F | \hat{H}_0 | F \rangle \tag{18}$$

$$E^{(1)} = \langle F | \hat{H}_1 | F \rangle \tag{19}$$

$E^{(0)}$ is the ground state energy of non-interacting Fermi gas and $E^{(1)}$ is the first order energy. In above equations, $|F\rangle$ is the normalized ground state wave function of the system. The ground state of the system is specified by the quantum variables $m = 0, n = 1, l$ [25].

CALCULATION OF ENERGY

In this section, we calculate the energy of spin-polarized metallic nanowire as follows. The Fermi momentum of spin-up particles is $l_F^{(+)}$ and Fermi momentum of spin-down particles is $l_F^{(-)}$. These are determined by the calculation of the expectation value of the number operator as follows,

$$\begin{aligned}
 N^+ &= \langle F | \hat{N} | F \rangle = \sum_{lmn\lambda=+1/2} \langle F | \hat{n}_{lmn\lambda} | F \rangle \\
 &= \sum_{lmn} \theta(l_F^{(+)} - l)
 \end{aligned} \tag{20-1}$$

$$\begin{aligned}
 &= \frac{L}{2\pi} \sum_{mn} \int_0^{l_F^{(+)}} dl \\
 &= \frac{L l_F^{(+)}}{2\pi} \Rightarrow l_F^{(+)} = 2\pi\rho^{(+)} = \pi\rho(1 + \xi) \\
 N^- &= \langle F | \hat{N} | F \rangle = \sum_{lmn\lambda=-1/2} \langle F | \hat{n}_{lmn\lambda} | F \rangle \\
 &= \sum_{lmn} \theta(l_F^{(-)} - l)
 \end{aligned} \tag{20-2}$$

$$\begin{aligned}
 &= \frac{L}{2\pi} \sum_{mn} \int_0^{l_F^{(-)}} dl \\
 &= \frac{L l_F^{(-)}}{2\pi} \Rightarrow l_F^{(-)} = 2\pi\rho^{(-)} = \pi\rho(1 - \xi)
 \end{aligned}$$

where $\theta(x)$ is the step-function.

We can write the Fermi momentum versus the total number density (ρ) [26],

$$\rho = \frac{N}{L} = \frac{l_F^{(+)} + l_F^{(-)}}{\pi} \tag{21}$$

Now, we calculate the expectation value of \hat{H}_0 ,

$$\begin{aligned}
 E^{(0)} &= \langle F | \hat{H}_0 | F \rangle \\
 &= \frac{N\hbar^2}{2m_e} \left[\left(\frac{3\pi}{4R} \right)^2 + \frac{(\pi\rho)^2 (1 + \xi)^3}{6} + \frac{(\pi\rho)^2 (1 - \xi)^3}{6} \right]
 \end{aligned} \tag{22}$$

and, we should calculate the expectation value of \hat{H}_1 ,

$$E^{(1)} = \langle F | \hat{H}_1 | F \rangle = \frac{1}{2} \sum_{lpq} \sum_{m_1 m_2 n_1 n_2 n_3 n_4} \sum_{\lambda_1 \lambda_2} PE \langle F | a_{l+q, m_1, n_1, \lambda_1}^+ a_{p-q, m_2, n_2, \lambda_2}^+ a_{p, m_2, n_2, \lambda_2} a_{l, m_1, n_1, \lambda_1} | F \rangle \quad (23)$$

where,

$$l = l_3, \quad q = l_4 - l_2, \quad p = l_4 \quad (24)$$

In above equation, we should consider the following relations,

$$\begin{aligned} 1) \quad l + q, \lambda_1 = l, \lambda_1 \quad ; \quad p - q, \lambda_2 = p, \lambda_2 \\ 2) \quad l + q, \lambda_1 = p, \lambda_2 \quad ; \quad p - q, \lambda_2 = l, \lambda_1 \\ 3) \quad m_1 = m_3 \\ 4) \quad n_1 = n_4 \quad ; \quad n_2 = n_3 \end{aligned} \quad (25)$$

We calculate the matrix element in Eq. (23) as follows,

$$\begin{aligned} \langle F | a_{l+q, m_1, n_1, \lambda_1}^+ a_{p-q, m_2, n_2, \lambda_2}^+ a_{p, m_2, n_2, \lambda_2} a_{l, m_1, n_1, \lambda_1} | F \rangle \\ = -\langle F | \hat{n}_{l+q, m_1, n_1, \lambda_1} \hat{n}_{l, m_1, n_1, \lambda_1} | F \rangle \\ = -\theta(l_F - |l + q|) \theta(l_F - l) \end{aligned} \quad (26)$$

Using $l \rightarrow p = l + \frac{q}{2}$, for $-l_F + \frac{q}{2} < p < l_F - \frac{q}{2}$, we have

$$\theta(l_F - |l + q|) \theta(l_F - l) = \theta\left(l_F - \left|p + \frac{q}{2}\right|\right) \theta\left(l_F - \left|p - \frac{q}{2}\right|\right) = 1 \quad (27)$$

Using the above calculations, we get the following relation for the total energy per particle of a spin polarized metallic nanowire in the presence of magnetic field,

$$\begin{aligned} \frac{E}{N} = \frac{E^{(0)}}{N} + \frac{E^{(1)}}{N} + \frac{E_M}{N} \\ = \frac{\hbar^2}{2m_e} \left[\left(\frac{3\pi}{4R} \right)^2 + \frac{(\pi\rho)^2}{3} + \frac{(\pi\rho)^2(1+\xi)^3}{6} + \frac{(\pi\rho)^2(1-\xi)^3}{6} \right] \\ + \frac{e^2}{2 \times 0.078(4\pi\epsilon_0)\pi^2\rho} \int_0^{2l_F^{(+)}} dq (2l_F^{(+)} - q) [(-0.0078) \times [K_0(\epsilon q)] + (0.0092) \times [K_0(2Rq)]] \\ + (0.018) \times \left[K_0 \left(\left(\frac{3\epsilon}{4} + \frac{R}{2} \right) q \right) \right] + (0.011) \times \left[K_0 \left(\left(\frac{\epsilon}{4} + \frac{3R}{2} \right) q \right) \right] \\ + (0.013) \times \left[K_0 \left(\left(\frac{\epsilon}{2} + R \right) q \right) \right] \} \\ + \frac{e^2}{2 \times 0.078(4\pi\epsilon_0)\pi^2\rho} \int_0^{2l_F^{(-)}} dq (2l_F^{(-)} - q) [(-0.0078) \times [K_0(\epsilon q)] + (0.0092) \times [K_0(2Rq)]] \\ + (0.018) \times \left[K_0 \left(\left(\frac{3\epsilon}{4} + \frac{R}{2} \right) q \right) \right] + (0.011) \times \left[K_0 \left(\left(\frac{\epsilon}{4} + \frac{3R}{2} \right) q \right) \right] \\ + (0.013) \times \left[K_0 \left(\left(\frac{\epsilon}{2} + R \right) q \right) \right] \} - \mu_e \xi B \end{aligned} \quad (28)$$

RESULTS AND DISCUSSION

We have calculated some thermodynamic properties of a metallic nanowire in the presence of magnetic field. Our results are as follows.

In Fig. 1, we have presented the ground-state energy per particle of spin-polarized metallic nanowire (with radius $R = 10$ nm) as a function of the density for different values of the magnetic field. For each value of the magnetic field, it is seen that the energy per particle is increased monotonically as the density increases.

However, the increasing rate of energy vs. density increases as the magnetic field increases. This indicates that at higher magnetic fields, the increasing rate of the contribution of magnetic energy vs. density is more than that at lower magnetic fields. In Fig. 2, we have given the energy of metallic nanowire for two different values of radius at magnetic field $B = 10$ T. We can see that for each density, the energy increases by increasing the radius.

In Fig. 3, the spin-polarization parameter corresponding to the equilibrium state of the metallic nanowire (with radius $R = 10$ nm) has been plotted as a function of the density for different values of the magnetic field. It is seen that at each magnetic field, the magnitude of spin-polarization parameter decreases by increasing the density.

Figure 3 also shows that for the magnetic fields less than 100 T, at high densities, the system nearly becomes unpolarized. However, for higher magnetic fields, the system has a substantial spin-polarization, even at high densities. Figure 4 shows a comparison between the spin-polarization of different radius of metallic nanowire. It is seen that at low densities, the spin polarization has a higher value as the radius increases. However, at high densities the spin polarizations of different radius become nearly identical.

From the energy of spin-polarized metallic nanowire, at each magnetic field, we can calculate the corresponding kinetic pressure ($P_{kinetic}$) using the following relation [27],

$$P_{kinetic}(\rho, B) = \frac{\rho^2}{\pi R^2} \left(\frac{\partial E(\rho, B)}{\partial \rho} \right)_B \quad (29)$$

Our results for the kinetic pressure of spin-polarized metallic nanowire (with radius $R = 10$ nm) vs. the density for different values of the magnetic field have been shown in Fig. 3.

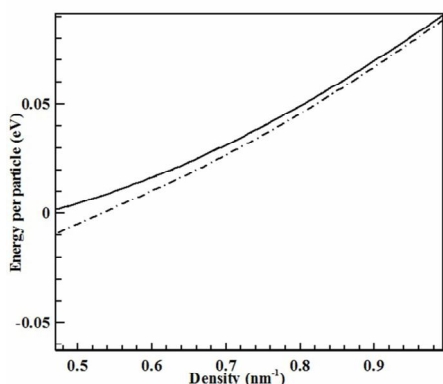


Fig. 1. The ground state energy per particle as a function of density at $B = 0$ (solid curve), 10 (dashed curve), 100 (dotted curve) and 1000 T (dash-dot curve) for $R = 10$ nm.

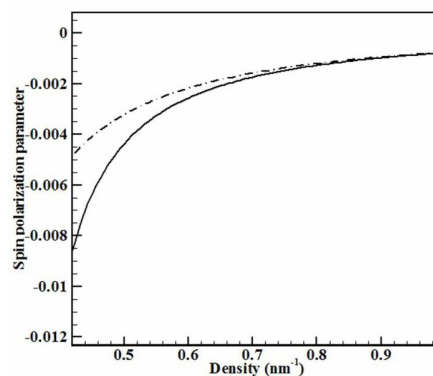


Fig. 4. The spin-polarization parameter at the equilibrium state of system as a function of density for $R = 5$ (solid curve) and 10 nm (dash-dot curve) at $B = 10$ T.

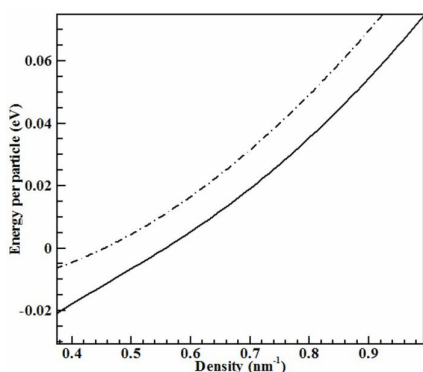


Fig. 2. The ground state energy per particle as a function of density for $R = 5$ (solid curve) and 10 nm (dash-dot curve) at $B = 10$ T.

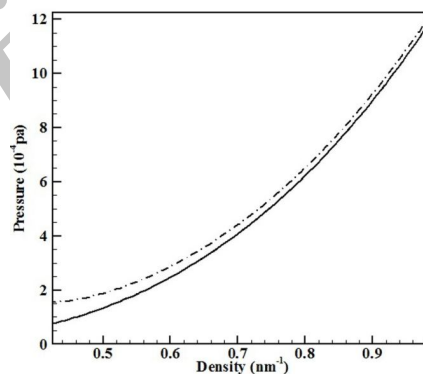


Fig. 5. The pressure at the equilibrium state of system as a function of density at $B = 0$ (solid curve), 10 (dashed curve), 100 (dotted curve) and 1000 T (dash-dot curve) for $R = 10$ nm.

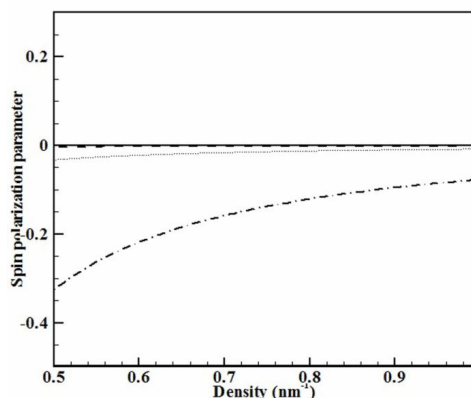


Fig. 3. The spin-polarization parameter at the equilibrium state of system as a function of density at $B = 0$ (solid curve), 10 (dashed curve), 100 (dotted curve) and 1000 T (dash-dot curve) for $R = 10$ nm.

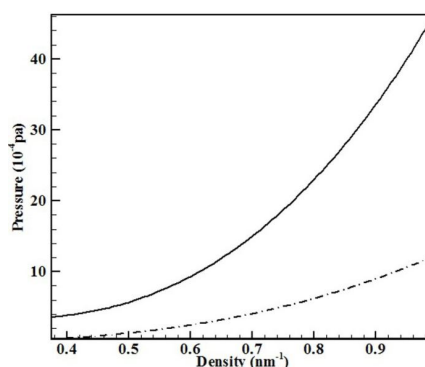


Fig. 6. The pressure at the equilibrium state of system as a function of density for $R = 5$ (solid curve) and 10 nm (dash-dot curve) at $B = 10$ T.

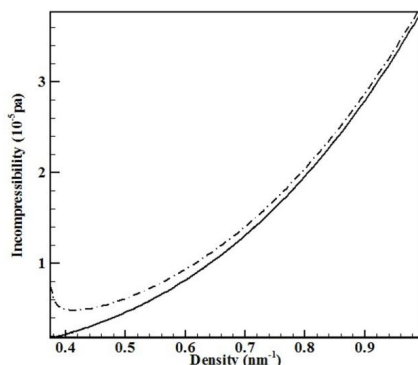


Fig. 7. The incompressibility of spin-polarized metallic nanowire vs. density at $B = 0$ (solid curve), 10 (dashed curve), 100 (dotted curve) and 1000 T (dash-dot curve) for $R = 10$ nm.

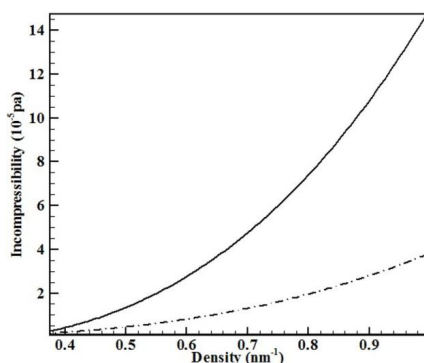


Fig. 8. The incompressibility of spin-polarized metallic nanowire vs. density for $R = 5$ (solid curve) and 10 nm (dash-dot curve) at $B = 10$ T.

It is obvious that as the density increases, the difference between the pressures of spin-polarized metallic nanowire at different magnetic field becomes more appreciable. Figure 5 shows that the pressures of small magnetic fields are nearly identical. A comparison is made between the equations of state of different values of metallic nanowire in Fig. 6. This indicates that by decreasing the radius, equation of state of metallic nanowire becomes stiffer. The incompressibility of system (α_T) can be computed from the following relation,

$$\alpha_T = \rho \left(\frac{\partial P(\rho, B)}{\partial \rho} \right)_B \quad (30)$$

In Fig. 7, we have plotted the incompressibility as a function of the density for the metallic nanowire (with radius $R = 10$ nm) in the presence of the magnetic field. It is seen that the incompressibility is increased as the density increases. However, the difference between the incompressibility of different magnetic fields is increased as the magnetic field increases. We have plotted the incompressibility of metallic nanowire for different radius at $B = 10$ T in Fig. 8. It is shown that the incompressibility decreases by increasing the radius, especially at high densities.

REFERENCES

- [1] H. Ohnishi, Y. Kondo, K. Takayanagi, *Nature* 395 (1998) 780.
 - [2] A.I. Yanson, G.R. Bollinger, H.E. van der Brom, N. Agrait, J.M. van Ruitenbeek, *Nature* 395 (1998) 783.
 - [3] P. Gambardella, A. Dallmeyer, K. Maiti, M.C. Malagoli, W. Eberhardt, K. Kern, C. Carbone, *Nature* 416 (2002) 301.
 - [4] N. Niluis, T.M. Wallis, W. Ho, *Science* 297 (2002) 1853.
 - [5] P. Gambardella, P. Blanc, M. Burgi, L. Kuhnke, K. Kern, *Surf. Sci.* 449 (2000) 93.
 - [6] P. Gambardella, A. Dallmeyer, K. Maiti, M.C. Malagoli, W. Eberhardt, K. Kern, C. Carbone, *Nature* 416 (2002) 301.
 - [7] O. Gulseren, F. Ercolessi, E. Tosatti, *Phys. Rev. Lett.* 80 (1998) 3775.
 - [8] Y. Cui, C.M. Lieber, *Science* 291 (2001) 851.
 - [9] X. Wang, Y.D. Li, *Am. Chem. Soc. J.* 124 (2002) 2880.
 - [10] L.Y. Zhang, D.S. Xue, J. Fen, *J. Magn. Mater.* 305 (2006) 228.
 - [11] M. Hayashi, L. Thomas, C. Rettner, R. Moriya, S.S.P. Parkin, *Nat. Phys.* 3 (2007) 21.
 - [12] H.X. Wang, Y.C. Wu, L.D. Zhang, X.Y. Hu, *Appl. Phys. Lett.* 89 (2006) 232508.
 - [13] S.H. Liu, J.B.H. Tok, J. Locklin, Z.N. Bao, *Small* 2 (2006) 1448.
 - [14] E.J. Menke, M.A. Thompson, C. Xiang, L.C. Yang, R.M. Penner, *Nat. Mater.* 5 (2006) 914.
 - [15] P.R. Kotiuga, T. Toffoli, *Physica D* 120 (1998) 139.
- A.J. Bennett, J.M. Xu, *Appl. Phys. Lett.* 82 (2003) 3304.

- [16] C.G. Jin, W.F. Liu, C. Jia, X.Q. Xiang, W.L. Cai, L.Z. Yao, X.G. Li, *Crystal Growth J.* 258 (2003) 337.
- [17] D.S. Xue, J.L. Fu, H.G. Shi, *J. Magn. Magn. Mater.* 308 (2007) 1.
- [18] J.C. Tung, G.Y. Guo, *Phys. Rev. B* 76 (2007) 094413.
- [19] J.T. Arantes, Antonio J.R. da Silva, A. Fazzio, arXiv:cond. mat/0608315v2.
- [20] G.H. Bordbar, L. Shamsavar, *J. Nanostruct. Chem.* 2 (2011) 193.
- [21] A.L. Fetter, J.D. Walecka, *Quantum Theory of Many-Body Systems* McGraw-Hill, 1971.
- [22] N.H. March, W.H. Young, Sampanthar, *The Many-Body Problem in Quantum Mechanics*, Cambridge University Press, 1967.
- [23] D. Pines, *The Many-Body Problem*, Benjamin, 1962.
- [24] J.M. Bergues, R. Betancourt-Riera, R. Riera, J.L. Marin, *J. Phys: Condens. Matt.* 12 (2000) 7983.
- [25] R.W. Robinett, *Eur. J. Phys.* 24 (2003) 231.
- [26] R.K. Pathria, *Statistical Mechanics*, Pergamon Press, 1988.

Archive of SID